Chapter 1
Introduction to Nuclear Magnetic Resonance (NMR) Methods

Allen W. Song

1.1 Introduction

Magnetic resonance imaging, commonly known as MRI, is perhaps one of the most important inventions in medical imaging and diagnosis. After the first image formation in the early 1970s (Damadian 1971; Lauterbur 1973), MRI has gone through a relatively quiet infancy, largely due to the lack of the necessary hardware. However, even since its first commercialization in the early 1980s, MRI has revolutionized the field of medical imaging, and evolved to be the gold standard for imaging brain and other soft tissues. In over two decades' time, MRI has affected most aspects of clinical diagnosis and treatment.

What makes MRI so powerful and popular? Two compelling reasons may be its ability to produce the clearest and most uniform images of organs, and its complete non-invasiveness. In this chapter, we will attempt to introduce MRI taking a mostly conceptual path, starting from the magnetic field and magnetization (M), signal generation and reception through proton resonance (R), to spatial encoding for generation of images (I). We will also introduce the versatility of MRI contrast generation, which can be used to emphasize different tissue characteristics. To convey both the elegance and the rigor of the MRI theory is a great challenge faced by teachers of MRI. As many prefer to learn by intuition and analogy, this section is written with very limited dependence on detailed equations, in order to provide the many readers a firm conceptual grasp on the key principles of MRI. It is hoped that readers will be able to understand the many basic but key concepts, so as to facilitate their continued reading further into this handbook.

A.W. Song, Ph.D. (✉)
Duke University Medical Center, Brain Imaging and Analysis Center,
Box 3918, Durham, NC 27710, USA
e-mail: allen.song@duke.edu

I.-Y. Choi and R. Gruetter (eds.), *Neural Metabolism In Vivo*,
Advances in Neurobiology 4, DOI 10.1007/978-1-4614-1788-0_1,
© Springer Science+Business Media, LLC 2012

1.2 Magnetic Field and Magnetization

1.2.1 Magnetic Field

MRI scanners typically use a strong static magnetic field to align certain nuclei within the human body (most commonly, hydrogen within water molecules) to allow mapping of tissue properties. Early MRI scanners used permanent magnets to generate magnetic fields, which are usually weak and hence lead to low MR signal. Another way of generating a magnetic field was discovered by the Danish physicist Oersted in 1820, when he demonstrated that a current-carrying wire influenced the direction of a compass needle below the wire, redirecting it perpendicularly to the direction of current. This relation was quantified later that year by the French physicists Biot and Savart, who discovered that magnetic field strength was in fact proportional to current strength, so that by adjusting the current in a wire (or sets of wires), one could precisely control field intensity. These findings led to the development of electromagnets, which generate their fields through tight coils of wire. Modern MRI scanners use superconducting electromagnets with wires cooled by cryogens (e.g., liquid helium) to reduce their temperature to near absolute zero.

To generate an extremely large magnetic field, one can inject a huge electric current into the loops of wire. For example, the very large electromagnets used to lift cars in junkyards have magnetic fields on the order of 1 T, similar to that in the center of a MRI scanner. To generate this field, they require enormous electrical power, as much as tens of kilowatts, and thus enormous expense. The use of superconductive materials in MRI scanners allows strong fields to be created without prohibitive cost. Coil windings are typically made of metal alloys such as niobium-titanium, which when immersed in liquid helium can reach temperature at ~4°K (−269°C), less than the critical temperature threshold (10°K) of this particular alloy. In this low-temperature state, the resistance in the wires disappears, thereby enabling a strong and lasting electric current to be generated with no power requirements, which in turn causes a very strong magnetic field.

Combining the precision derived from numerical optimization of the magnetic coil design and the strength afforded by superconductivity, modern MRI scanners can have homogeneous and stable field strengths in the range of 1–9 T for human use and up to 20 T for animal use. In comparison, the earth's magnetic field is approximately 0.00005 T. A typical MRI scanner is shown in Fig. 1.1, the tubular main structure contains the superconductor main magnet, as well as the necessary coils for generating signal and creating images (discussed in detail in the following sections). Since maintaining a field using superconductive wiring requires no electricity, the static fields used in MRI with superconducting magnets are always active, even when no images are being collected. For this reason, these static fields present significant safety challenges, as will be discussed later in this chapter.

Magnetic field creates magnetization in certain objects. A classic demonstration of magnetism can be created by sprinkling some iron filings around a standard bar magnet. The filings clump most densely around the poles of the magnet but also form a series of

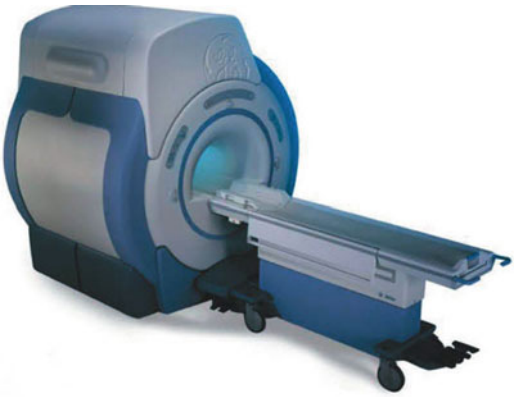

Fig. 1.1 A typical MRI scanner

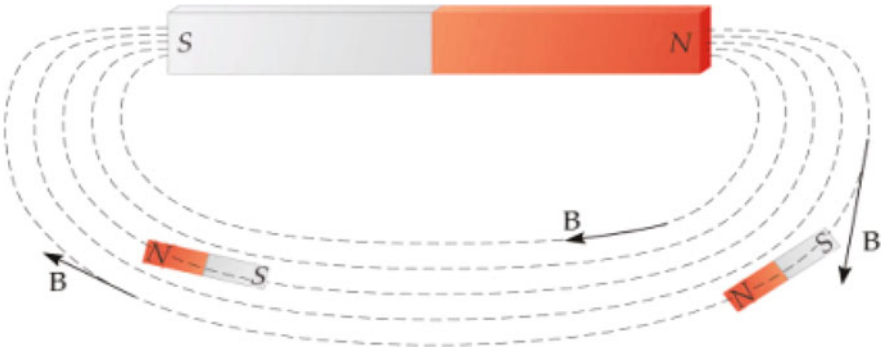

Fig. 1.2 Alignment of bar magnets in an external magnetic field

arcs between the poles. These arcs run along the field lines of the magnet and result from the tendency of individual iron filings to align with the external field. Figure 1.2 presents a schematic illustration of this alignment, which is driven by the principle of energy minimization. Just as massive objects in a gravitational field tend to lower their energy by falling rather than remaining suspended in midair, magnetically susceptible objects in a magnetic field will orient along the field lines rather than across them. For macroscopic objects, like oxygen canisters, the alignment process is known as torsion and presents safety issues. More severely, when placed near magnets where the magnetic field changes are steep, these large magnetic objects will experience tremendous forces attracting them toward the magnets, resulting in the dangerous "projectile" effect. The pattern of field lines is a mathematical description of the contours of the magnetic field, with the density of lines in a location indicating the local strength, or flux, of the magnetic field. In magnetic resonance imaging, the main magnetic field of the scanner is often indicated by the symbol $\mathbf{B}_0$.

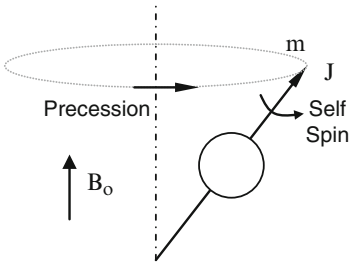

Fig. 1.3 Illustration of precession motion for self-spinning protons

The effect of a magnet on iron filings is intuitive, as they will be magnetized and therefore align with the direction of the magnetic field. What happens if we place biological tissue in a magnetic field?

1.2.2 The Effect of Magnetic Field on Protons in Biological Tissue

To understand the effect of magnetic field on biological tissue, e.g. human body, we will need to first characterize its composition. An average person who weighs 150 lbs. contains approximately 5×10^{27} hydrogen protons (because of the high water content). As such, protons are by far the most dominant nuclei in the human body, and are the main sources of signal for the vast majority of the MRI exams. We will thus focus on hydrogen protons in this introduction chapter. It is worth noting that many other nuclei with odd number of protons and atomic mass (i.e. simultaneous possession of magnetic moment and angular momentum), such as ^{13}C, ^{19}F, ^{23}Na, and ^{31}P, can also generate MR signal.

Under normal conditions, thermal energy causes the proton to spin about itself. The spin motion of a proton has two effects. First, because the proton carries a positive charge, its spin generates an electrical current on its surface, just as a moving electrical charge in a looped wire generates current. This loop current creates a small proton magnetic field and a torque when the proton is placed within an external magnetic field; the strength of the proton magnetic field or the maximum torque (i.e. when placed orthogonally into an external magnetic field) per unit magnetic field strength is called the magnetic moment, or **m**. Second, because the proton has an odd-numbered atomic mass (i.e., 1), its spin results in an angular momentum, or **J**. Both **m** and **J** are vectors pointing in the same direction, along the spin axis.

When placed in a magnetic field, protons, like iron filings, would change their orientation because of their magnetic moment. However, instead of turning to align with the magnetic field, the spinning protons initiate a gyroscopic motion known as precession (Fig. 1.3) because of their simultaneous possession of angular momentum. To understand precession, imagine a spinning top on a desk. The top does not spin perfectly upright; instead its axis of rotation traces a circle perpendicular to the

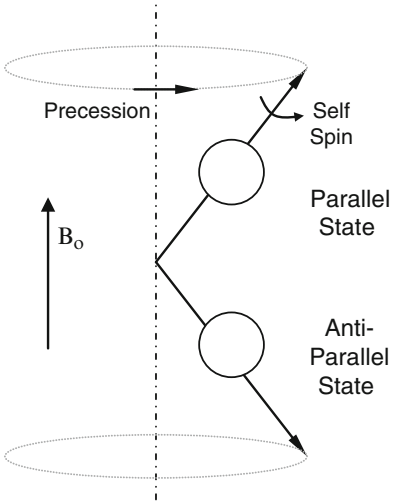

Fig. 1.4 Parallel and antiparallel states of precession

earth's gravitational field. At any moment in time the top is tilted from the vertical, but it does not fall. Why does the top spin at an angle? Spinning objects respond to applied forces by moving their axes in a direction perpendicular to the applied force. A bicycle, for example, is very stable and resists falling over at high speeds, due to the gyroscopic effects of its spinning wheels. When a rider leans to one side, the moving bicycle will not fall but will instead turn in that direction. Similarly, a spinning top turns its axis of rotation at an angle perpendicular to the force exerted by gravity, so that the top precesses in a circle around a vertical axis. Because the precession frequency is determined by the type of nucleus, all protons precess at the same frequency when experiencing the same strength of magnetic field. This characteristic frequency is called the Larmor Frequency.

Interestingly, there are two states for precessing protons: one parallel to the magnetic field and the other antiparallel (Fig. 1.4). Protons in the parallel state have a lower energy level, while protons in the antiparallel state have a higher energy level. The idea of two energy states can be understood by imagining a bar that can rotate around one end. There are two vertical positions for the bar: one balanced above the pivot point and one hanging down from the pivot point. The balanced position is a high-energy state and is not very stable; even a small perturbation may tip the bar over and cause it to fall to the hanging position. The only way to keep the bar in a balanced position is to apply an external force that can counteract gravity. That is, energy must be applied to keep the bar in the high-energy state. The hanging position is much more stable, since it is at the minimum energy level for this system. For protons, the parallel (low-energy) state is slightly more stable, so there will always be more protons in the parallel state than in the antiparallel state, with the relative proportion of the two states dependent upon temperature and the strength of the magnetic field. At room temperature in the earth's magnetic field, roughly equal numbers of protons are in the two energy states, with slightly more in the parallel state.

If the temperature increases, some protons will acquire more energy and jump to the antiparallel state, diminishing but never reversing the already small difference between the two levels. Conversely, if the temperature decreases, protons will possess less energy and even more will stay at the lower energy level. This relationship is described by the Boltzmann distribution $\frac{P_p}{P_a} = e^{\frac{\Delta E}{k_B T}}$, where P_p and P_a are the proportions of protons in parallel and anti-parallel states, respectively, here $P_p + P_a = 1$, T is the absolute temperature, ΔE is the energy difference between the parallel and anti-parallel states, k_B is the so-called Boltzmann constant (1.3806×10^{-23} J/K).

The discrete energy difference between the two states (ΔE) can be measured experimentally. Interestingly, this energy difference is equal to the energy possessed by photons at the precession frequency under the same magnetic field strength. As such, the precessing protons may absorb energy from oscillating electromagnetic fields at the same frequency and change their states. This phenomenon, which was confirmed by the first magnetic resonance experiment carried out by Rabi's laboratory in the 1930s (Rabi et al. 1938), provides a basis for unifying the quantum and classical mechanics concepts in the context of proton excitation discussed later. The precession frequency (ω) is known as the Larmor frequency, and defined by the Larmor equation $\omega = \gamma B_o$ where γ is the gyromagnetic ratio and B_o the magnetic field strength. The gyromagnetic ratio differs for different nuclei, for hydrogen proton, the ratio is 2.67×10^8 radian/T (or 42.58×10^6 cycles/T).

1.2.3 Magnetization of Biological Tissue

It is important to emphasize that MR techniques do not detect just a single hydrogen nucleus, but instead measure the net magnetization of all protons in a volume. Because of the enormous number of protons within even the smallest volume, their transverse components will tend to cancel out, and there will be no net magnetization perpendicular to the main magnetic field (i.e. in the transverse plane). The net magnetization, known as **M**, is thus a vector whose orientation is along the longitudinal direction parallel to the main field, and whose magnitude is proportional to the difference in the number of the proton spins in the parallel and antiparallel states. The more protons at the parallel state, the bigger the **M** (Fig. 1.5), and in turn the larger the MR signal.

Because the proportion of parallel-state protons increases with decreasing temperature, as indicated by the Boltzmann equation, one way to increase the net magnetization is to reduce the temperature. While theoretically possible, this approach is impractical, given that the temperature would need to be lowered by many degrees Celsius to observe a noticeable increase in net magnetization. A more feasible approach is to increase the strength of the external field, based on the Zeeman effect – which states that the net magnetization is proportional to the magnetic field strength. Just as it would be more difficult to lift an object in a stronger gravitational

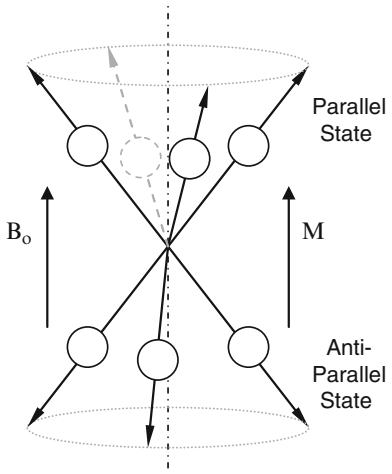

Fig. 1.5 Small difference in parallel and antiparallel protons create a net magnetization M

field than in a weaker gravitational field, it takes more energy to shift from a low-energy state to a high-energy state when the external magnetic field is stronger. Therefore, to increase the net magnetization in a sample (i.e., the proportion of parallel protons), one can place that sample in a very strong magnetic field.

Both the increase in net magnetization and the energy difference between the two states are linearly proportional to the strength of the magnetic field. The combination of these two factors means that the amplitude of the measured MR signal increases quadratically with field strength (e.g., the MR signal is four times as large in a 3 T scanner than in a 1.5 T scanner). Thus, even though the noise in the MR signal increases linearly with field strength, there remains a substantial signal-to-noise advantage to having stronger MRI scanners. For this reason, scanners commonly used for MRI in humans have continually progressed from a field strength of 1.5 T or less in early years, to the wide adoption of 3 T or even higher fields at the present time.

The net magnetization of protons within a volume provides the basis for MR signal generation, but net magnetization itself cannot be measured directly under equilibrium conditions. To understand this principle, recall the analogy of an object whose weight you are trying to estimate. You cannot know the object's weight just by looking at it; instead, you have to lift it. By lifting the object, you perturb its equilibrium state in the gravitational field, and the force observed in reaction to that perturbation allows you to estimate its weight. Measuring net magnetization of protons in a magnetic field is no different; you must perturb the equilibrium state of the protons and then observe how they react to the perturbation. Just as lifting perturbs the position of an object, excitation perturbs the orientation of the net magnetization, which allows its precession to be visible. Because the net magnetization is the sum of all the individual protons, it would naturally precess at the same characteristic frequency, the Larmor frequency.

1.3 Excitation and Reception of MR Signal

Following Rabi's experiments in magnetic resonance, independent groups led by Purcell and Bloch detected MR signal using radiofrequency transmitter and receiver coil (Purcell et al. 1946; Bloch 1946). The phenomenon was then labeled nuclear induction. The early work by these MR physicists earned them respective Nobel Prizes (Rabi in 1944; Purcell and Bloch in 1952), but more importantly, helped establish a core set of physical principles for MR signal generation. These principles are elegant in their simplicity, in that they begin with the properties of atomic nuclei and progress to the signal measured using MRI. Yet, they are also rigorous. In this section, we will introduce the concept of excitation and signal reception using resonating **radiofrequency (RF) coils**, as well as signal relaxation mechanisms.

1.3.1 Radiofrequency Coils

While a strong magnetic field establishes magnetization, it in itself does not produce any MR signal. MR signal is actually produced by the clever use of two types of RF coils, known as transmitter and receiver coils, that resonate at the same frequency as the precessing hydrogen magnetization generated by the main magnet. This process gives the name "resonance" to magnetic resonance imaging. Unlike the static magnetic field, the radiofrequency fields are turned on briefly during periods of the imaging process.

When the RF coils send electromagnetic waves into the body, in a process known as **excitation**, protons at lower energy state (i.e. parallel state) absorb energy and change to higher energy state (i.e. anti-parallel state). When the radiofrequency pulse ends, the protons then release the energy absorbed during excitation. The resulting release of energy can be detected by the RF coils, in a process known as **reception**. One can think of the measurement of MR signal through excitation and reception as analogous to the weighing of an object by lifting and releasing it in a gravitational field. If an object sits motionless on a supporting surface, so that it is in an equilibrium state with respect to gravitational force, we have no information about its weight. To weigh it, we first lift the object to give it potential energy and then release it so that it transfers that energy back into the environment. The amount of energy it releases, whether through impact with a surface or compression of a device like a spring (e.g., in a scale), provides an index of its weight. In the same way, we can perturb the magnetic properties of atomic nuclei (excitation) and then measure the amount of energy returned during their recovery back to an equilibrium state.

The amount of energy that can be transmitted or received by the radiofrequency coils depends upon the distance from the sample being measured. In the case of fMRI, the radiofrequency coils are typically placed immediately around the head, either in a surface coil (a coil that only covers a partial area) or volume coil (a coil that encompasses the entire volume) arrangement. Recent advances in coil design combine the best features of both coil types by using a volume coil for exciting the imaging volume and a set of surface coils for receiving the MR signal. If multiple

Fig. 1.6 An eight-channel array RF coil for head imaging

receiver coils are arranged in an overlapping pattern (e.g., phased array coils), the spatial coverage of a single coil can be increased considerably while the high sensitivity of the coils is still maintained. Shown in Fig. 1.6 is an example of a head coil array with eight-channel surface coils. Though sensitivity does change somewhat across the image, the use of multiple receiver coils is an increasingly important technique in fMRI.

1.3.2 Excitation and Signal Reception

We learned that protons can take either a high-energy state or a low-energy state within a magnetic field. The transitions between these two states are sparked by the perturbation of externally applied energy equal to the energy difference between the two states, in the form of the radiofrequency pulse transmission. For example, a proton in the low-energy state can jump to the high-energy state by absorbing energy from the radiofrequency pulse. Such a perturbation changes the probabilistic distributions of the high-energy and low-energy protons, with the rate of change favoring that going from the more populated state to the less populated state. Let's begin with an original condition, where there are more protons at the lower energy level, some protons in the low-energy state absorb the appropriate amount of energy and change to the high-energy state, in a process known as excitation (Fig. 1.7a). At any point when the electromagnetic waves (RF pulses) are turned off, the protons stop changing states. For example, the RF pulse can stop at the time when there are equal numbers at the two states (zero net longitudinal magnetization). Alternatively, in the classical mechanical description, it is the so-called 90 degree RF pulse – as the original net magnetization can be viewed as a vector in the longitudinal direction, and zero net longitudinal magnetization is only possible when the vector turns 90 degrees into the transverse plane. Importantly, the most common radiofrequency pulses for excitation are often designed to fully transition the longitudinal magnetization to the transverse plan, and the most efficient one of such is the 90 degree pulse.

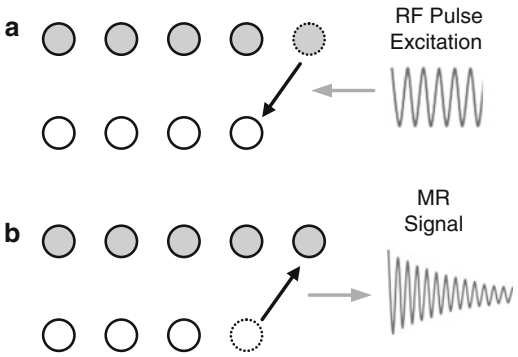

Fig. 1.7 Schematic illustration of proton excitation (**a**) and MR signal generation (**b**)

Since excitation disrupts the thermal equilibrium by creating more high-energy protons than would otherwise be present, immediately after excitation ceases the excess protons at the higher energy level return to the lower level (Fig. 1.7b) to reestablish the equilibrium proportions of energy states. During the time when protons in the high-energy state fall back to the low-energy state, they emit photons back to the system, with energy equal to the energy difference between the two states. Alternatively, in classical mechanics view, the precessing transverse magnetization will broadcast electromagnetic waves oscillating at the Larmor frequency, inducing a sinusoidally-varying voltage in the radiofrequency receiver coil tuned to the same frequency and placed perpendicular to the transverse plane. Because the frequencies of excitation and reception are both at the same Larmor frequency determined by the energy difference between the two states, often the same radiofrequency coil is used for both processes.

The critical concept underlying excitation and reception is that of the change in net magnetization from the longitudinal axis to the transverse plane. When the net magnetization is along the longitudinal axis, the individual protons' precession cannot be measured in detector coils. But, when the net magnetization is tipped to the transverse plane via excitation, its precession now generates an oscillating electric current in receive coils within the scanner.

1.3.3 MR Signal Relaxation Mechanisms

The MR signal detected through receiver coils does not remain stable forever. It changes in two ways after proton excitation and during signal reception: the transverse magnetization quickly loses coherence and the longitudinal magnetization will slowly recover. Together, these changes in the MR signal over time are called relaxation, with the former termed transverse relaxation (or transverse decay), also known as spin-spin relaxation, and the latter longitudinal relaxation (or longitudinal recovery), also known as spin-lattice relaxation. Both mechanisms constrain MR imaging parameters yet allow the generation of different types of images.

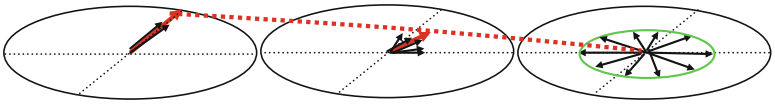

Fig. 1.8 Illustration of transverse (T2) relaxation (decay): the net magnetization vector (in *red*), which is the sum of individual spins (in *black*), decays in time (from *left* to *right*)

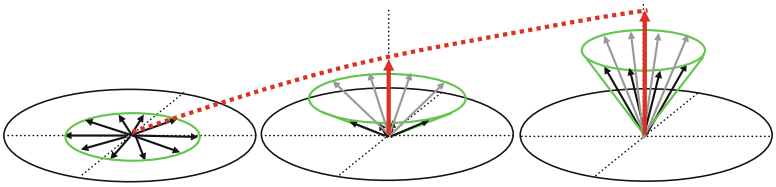

Fig. 1.9 Illustration of longitudinal (T1) relaxation (recovery): the net magnetization vector (in *red*), which is the sum of individual spins (in *black*), recovers in time (from *left* to *right*)

After excitation, the net magnetization is tipped from the longitudinal axis into the transverse plane. Because the net magnetization reflects the vector sum of many individual proton spins, its amplitude depends on the coherence between those spins, specifically that they precess at the same phase and with the same frequency. Yet, over time, they lose coherence. Spatially proximate spins may interact via dipolar coupling, analogously to bumper cars on a track, causing some to precess at higher frequencies, and some lower. This causes a loss of phase coherence among the protons, which leads to an exponential decay in the MR signal that is described by a time constant called T_2.

In addition, any spatial inhomogeneities in the magnetic field will cause different protons to experience different magnetic fields over time, changing their rate of precession. This effect is additive to the T_2 decay, and thus the combined transverse relaxation effect of proton spin-spin interactions and magnetic field inhomogeneity is described by the time constant T_2^*. As a result of T_2 or T_2^* decay, spins lose coherence relatively quickly (typically within a few tens of milliseconds), resulting in a diminishing net magnetization in the transverse plane (Fig. 1.8).

At the same time while spins are losing coherence due to spin-spin interactions, energy that was absorbed during excitation is emitted as radiofrequency waves that can be detected as MR signal. As the system loses energy, it recovers back to the same state as before the excitation – with the net magnetization pointing along the longitudinal axis (Fig. 1.9). The longitudinal recovery is relatively slow, typically on the order of a few hundreds of milliseconds to a few seconds, and is described by the time constant $\mathbf{T_1}$. The values of T_1 and T_2 for a spin system depend upon the kinds of substance present.

Although the T_1 and T_2 relaxations are plotted as separate processes, which is an approximation based on their largely different time constants (e.g. T_1 is usually one order of magnitude larger than T_2), these two relaxations occur simultaneously. And thus, for practical purposes they can be considered to make separate contributions

to the MR signal. Depending upon when an image is acquired during the relaxation process, either T_1 or T_2 (or a combination) will determine the amplitude of the recovered MR signal and thus the intensity of the image. By choosing appropriate imaging parameters, different tissues (e.g. gray vs. white matter) will produce different intensities (and hence contrast), so that investigators can differentiate them for diagnostic or research purposes. In addition, the speed of T_1 recovery influences the rate at which images can be collected, in that the T_1 recovery renews the longitudinal magnetization so that it can be again excited.

1.4 MR Image Formation

The fundamental innovation that made MRI possible was the introduction of superimposed gradient magnetic fields (spatially varying magnetic fields) (Lauterbur 1973; Mansfield 1977). Because of the dependency of the precession frequency on the strength of magnetic field, gradient magnetic fields will lead to spatially dependent distribution of precession frequencies. By differentiating these frequencies according to their spatial locations, we can generate maps (or images) of proton distribution. This innovation has such a large impact in the field of MRI that it has earned Paul Lauterbur and Peter Mansfield a share of the Nobel Prize for Physiology and Medicine in 2003.

1.4.1 Gradient Coils

The combination of a static magnetic field and a radiofrequency coil allows detection of MR signal, but MR signal alone cannot be used to create an image. The fundamental measurement in MRI is merely the amount of current through a coil, which in itself has no spatial information. By introducing magnetic gradients superimposed upon the strong magnetic field, **gradient coils** provide the final component necessary for imaging. The purpose of a gradient coil is to cause the MR signal to become spatially dependent, so that different locations in space contribute differently to the measured signal over time. The gradient fields can be turned on and off, briefly after the excitation process, to provide spatial encoding needed to resolve an image.

To make the recovery of spatial information along any given direction, a gradient coil is used to generate a magnetic field that increases in strength along that particular spatial direction. To resolve all three dimensions, typically three gradient coils are required. Shown in Fig. 1.10 is a schematic illustration of the gradient magnetic fields along x, y and z directions. Note that the gradient direction indicates the direction of change of the magnetic field, not the direction of the field itself (which always points along z).

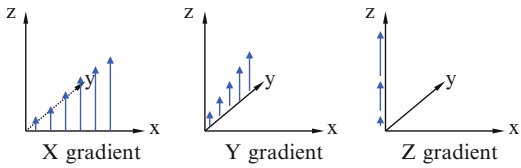

Fig. 1.10 Illustration of gradient fields along x, y and z directions. The vectors (in *blue*) indicate the strength and direction of the magnetic field

The strength of the gradient coil is a function of both the current density and the physical size of the coil. Increasing the current density by increasing the electrical power supplied to the coil produces a stronger gradient field. Reducing the size of the coil, so that a given current travels through a smaller area, also produces a stronger gradient field.

Naturally, since gradient fields along any direction will modulate the precession frequency, one cannot turn on all gradient fields at the same time and hope to resolve spatial information along all directions (as turning on all gradient fields will lead to a single diagonal direction). Instead, a sequence of gradient field actions, along with radiofrequency pulses, is used to create an MR image. We hereby break down MR image formation into the following components, which often occur in temporal order. First, we select a slice (slice selection) to reduce the dimension from 3D to 2D, then we systematically resolve the remaining two dimensions (frequency encoding and phase encoding) within this selected slice to obtain a final image.

1.4.2 Slice Selection

A useful practice in image formation is dimension reduction. Thus, a common first step in producing an MR image is to generate signal only from, for example, a head slice instead of from the whole head - this process is termed slice selection.

The proton excitation principle that we have learned in the last chapter requires a resonance between the precessing proton spins at the Larmor frequency and the RF pulse, that is, the frequency of the RF pulse and spin precession must match each other. In a perfectly uniform magnetic field, all spins within the same field will be excited by the RF excitation pulse at the Larmor frequency, obviously this excitation scheme has no spatial selectivity.

Now let's think of an extreme case where three discrete Larmor frequencies are seen in three contiguous, parallel slabs. In order to select the middle slab, we need to set the frequency of the RF excitation pulse to match that of the middle slab. As such, the spins in the middle slab are "on resonance" with the excitation pulse, thereby changing its state from the longitudinal to the transverse condition and positioning themselves to emit MR signal; the outer slabs are unaffected.

In reality, the frequency distribution in space is not discrete. Indeed, if a spatial gradient field (Gz) is turned on along the slice direction (e.g. z direction), it will result in a continuously changing field as illustrated by arrows (i.e. spin phases) rotating at different rates and angles (Fig. 1.11). Thus a particular slice in space will

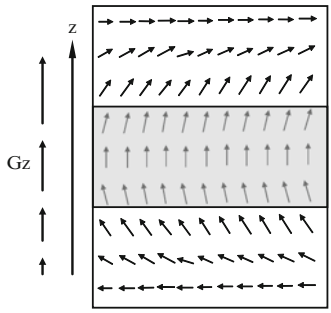

Fig. 1.11 Schematic illustration of slice selection along z direction by matching the frequencies of the RF excitation pulse and proton resonance within the slice

correspond to a band of Larmor frequencies, as shown in dark gray. To match this frequency band, the excitation RF pulse will need to have the same corresponding frequency range as well. Thus, if we know the spatial gradient field along the slice direction, or the slice-selective gradient, as well as the slice thickness, we can determine the resonance frequency range as the product of these two quantities with a scaling constant. Conversely, if we know the bandwidth of the RF excitation pulse, we can calculate the slice thickness. This relationship can be simply described by the following equation: $\omega \pm \frac{\Delta\omega}{2} = \gamma G(x \pm \frac{\Delta x}{2})$, here $\gamma$is the gyromagnetic ratio, G is the slice-selection gradient strength, ω and $\Delta\omega$ are the center frequency of the excitation pulse, x and Δx are the position and thickness of the slice.

To this end, we have discussed, conceptually, how slice selection is carried out. The key concept of matching the precessing frequency within the slice (controlled by the spatial gradient) to the frequency of the excitation RF pulse is the basic foundation for slice selection. Immediately after the slice selection, the protons are excited and will undergo T_1 and T_2 relaxation processes. As discussed in the previous chapter, T_2 relaxation will lead to a loss of spin coherence in the transverse plane, and T_1 relaxation will lead to an exponential recovery back to the original state – both resulting in decay of MR signal. As such, the subsequent spatial encoding steps (e.g. frequency encoding) for image formation will need to be quickly carried out after the slice selection.

1.4.3 Frequency Encoding

Once a 2D slice is selected, the next task is to resolve the spatial information within the remaining two dimensions. Because MR signal is acquired from the entire slice, inherently there is no spatial information. To achieve spatial resolution, here we introduce a procedure that involves two intertwined processes, frequency encoding and phase encoding, both taking advantage of the gradient fields. These two processes, however, can often be analyzed independently as they are separated in time. In this section, we will first focus on the concept of frequency encoding.

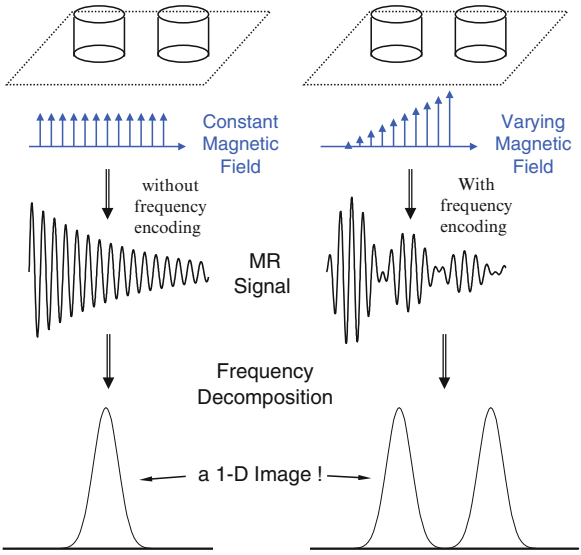

Fig. 1.12 Illustration of the use of gradient field (*right column*) to resolve spatial location

Let's first consider a simple case: imagine we need to make a one dimensional image of two elements, e.g. two thin vials of water. In the absence of gradient field (left column, Fig. 1.12), the resonance frequencies of these two vials are uniform, as a result, the detected analog MR signal from each water-filled vial will oscillate at the same frequency, with a decaying profile due to the aforementioned transverse relaxation mechanism. The frequency spectrum of this single-frequency oscillation will then show a single peak, at the resonance frequency with its width inversely proportional to the transverse relaxation constant. In the presence of a gradient field along the direction of these two vials, however, the two thin vials will have two distinct resonance frequencies, resulting in an oscillating MR signal with a pattern of beat frequency but still with an exponentially decaying envelope due to transverse relaxation. After a frequency decomposition procedure, we can resolve these two resonance frequencies with two peaks (right column, Fig. 1.12). By calibrating the separation of these two peaks and making it correspond to the physical distance between the two vials through the knowledge of the applied gradient field, we just generated a 1D image of these two vials!

While it is straightforward to record the analog MR signal continuously to characterize the two frequency components as demonstrated earlier, it is not always the most efficient way to collect data. To improve the efficiency, often only a limited number of discrete data points are collected, and they are used subsequently to resolve the two discrete frequencies - in fact, only two discrete points are needed. Specifically, let's assume the intensities of the two vials are A and B (which are unknown), the goal of making an MR image is then to find these two quantities. Let's consider collecting data under a spatial gradient G in the x direction. Although the protons in these two vials precess at different frequencies, at time 0, they start off at the same phase. This can be better depicted by vectors: considering two vectors

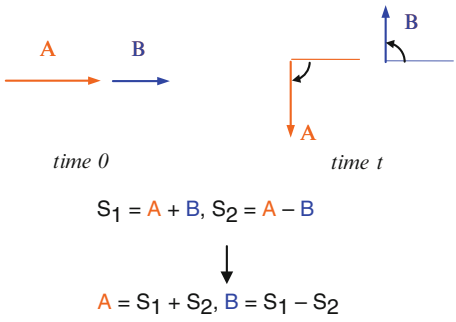

Fig. 1.13 An example of resolving the signal amplitude from two voxels (**a** and **b**) along one dimension

(with intensities A and B), initially pointed along the same direction, which would result in an original total signal $S_0 = A + B$. After some time *t*, different protons at different spatial positions will build up leads and lags in phase because of their different precessing frequencies (frequency × time = phase), and thus, the received signal will have a new intensity C that is governed by the sum of the vectors of A and B. With these two known intensities, and since the precise rotation angles of these two vectors can be determined by the gradient field we applied, we can determine the values of A and B.

To better visualize the frequency encoding process, we can even arrange to acquire data at a specific time point such that the rotation angles of the two vectors are $-\pi/2$ and $\pi/2$, respectively, which will lead to the simplest form of signal representation to solve for the two spatial points (with intensities A and B), as shown in Fig. 1.13.

We can expand our analysis from these two vials to more complex (and realistic) examples. If we have *n* image elements (known as voxels) in space with corresponding intensities (A_1, A_2, … A_n). As usual, these intensities are unknown before the image is formed. We thus need to resolve these intensities to form the final image. From the previous simpler example of resolving two points in space, and by way of extrapolation, we should collect *n* time points under a gradient magnetic field at time t_1, t_2, … t_n, leading to *n* distinct data points with their respective phase angles distributed evenly over a 2π range, leading to *n* uncorrelated signals of S_1, S_2, … S_n. From these *n* known data points and the gradient amplitudes and durations, we will be able to resolve the *n* intensities of each element along this dimension and form a one dimensional image.

1.4.4 Phase Encoding

The final step is then to resolve the second dimension within the selected slice – which will, again, involve the use of a magnetic field gradient. The general term for resolving this second spatial dimension is called phase encoding.

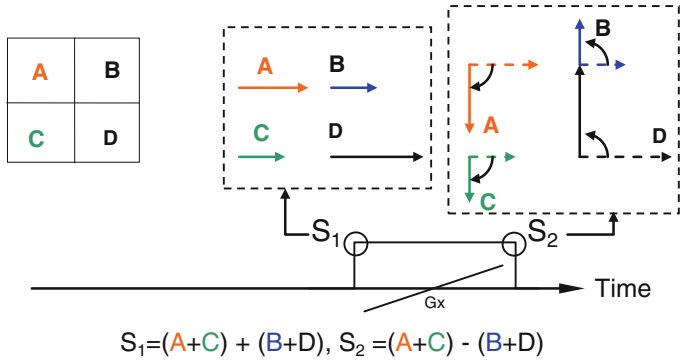

Fig. 1.14 MR data acquisition during frequency encoding, illustrated using a 2×2 matrix

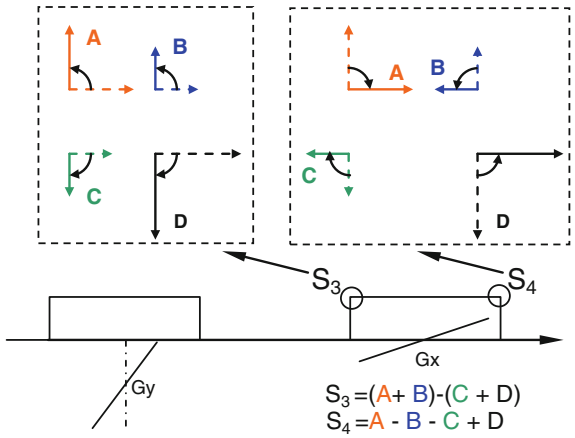

Fig. 1.15 MR data acquisition after phase encoding, illustrated using a 2×2 matrix

For simplicity, we again consider a 2×2 case, with four elements of unknown intensities A, B, C, and D. To resolve the *x* direction, we first perform frequency encoding, as described above. Because there are only two different spatial locations along the *x* direction, we just need to acquire two data points. Similar to the acquisition process in Fig. 1.13, we can collect MR data S_1 and S_2 as illustrated in Fig. 1.14.

We learned previously that we cannot simply turn on the *y* gradient at the same time as the *x* gradient to resolve two dimensional spatial information. Instead, we would first need to complete one gradient, say *y* gradient, before the MR signal is acquired (as opposed to after the MR signal acquisition which serves no purpose). This operation will pre-build phase lags and leads to different voxels according to their respective positions along the *y* direction. The amount of phase accumulations is then carried forward into the frequency encoding process to encode the spatial information in the *y* direction. This process, as illustrated in Fig. 1.15, is the most commonly used method in resolving the second dimension, and known as phase

encoding because it builds up a pre-determined amount of phase for a given voxel. The two additional data points, S_3, and S_4, collected after the phase encoding step, along with the previously collected two points, S_1 and S_2, are independent and can be used to resolve four individual intensities A, B, C and D.

While logically it appears simple to directly solve N×N unknowns with N×N known quantities, N being the imaging matrix size, in practice, it can be quite computationally intensive and often impractical for routine use. For example, a 256×256 matrix would require solving 65536 unknowns – which would greatly reduce the image reconstruction speed. Thus, for modern MRI, the two spatial dimensions are resolved not by linear algebra, but rather by a more efficient mathematical process known as the Fourier Transformation (FT) (Ernst et al. 1987). By reorganizing the acquired two-dimensional MRI raw data directly from the scanner, it would become identical to the FT of the actual image. Thus, by carrying out a 2D inverse FT, an MR image can be efficiently resolved. FT is the most prevalent reconstruction technique in modern MRI.

1.4.5 Versatile Contrasts in MR Images

MRI is extraordinary, compared to other methods for medical imaging, in generating versatile and quantitative contrasts in images. Image contrast can be created to emphasize different and unique tissue characteristics. Because of the importance of MRI in specific contrast generation, we introduce in this section several different but important contrast mechanisms. **Static contrasts** are sensitive to the type, number, relaxation and resonance properties of atomic nuclei within a voxel. Typical static contrasts are based on density (e.g., proton density), relaxation time (e.g., T_1, T_2, T_2^*), chemical concentration (e.g. lactate in the brain), and even content of a particular molecular type (e.g., macromolecules). Many of these static contrasts can be used to assess anatomy. In comparison, **motion contrasts** are sensitive to the movement of atomic nuclei. Typical motion contrasts provide information about the dynamic characteristics of the proton pools in the brain, such as blood flow through MR angiography, water diffusion through diffusion-weighted imaging, or capillary irrigation through perfusion-weighted imaging. Many of these motion contrasts can be used to assess function.

In the following sections, we will briefly introduce the various contrasts to appreciate the versatility of MRI in contrast generation. We will begin with several common static contrasts, followed by motion contrasts. More details on the many useful MR contrasts can be found in later chapters, and in several other textbooks on MRI (Stark and Bradley 1992; Haacke et al. 1999).

1.4.5.1 Proton-Density Contrast

One of the simplest forms of MR contrast is proton density imaging. The net magnetization of each voxel is composed of individual protons within that voxel.

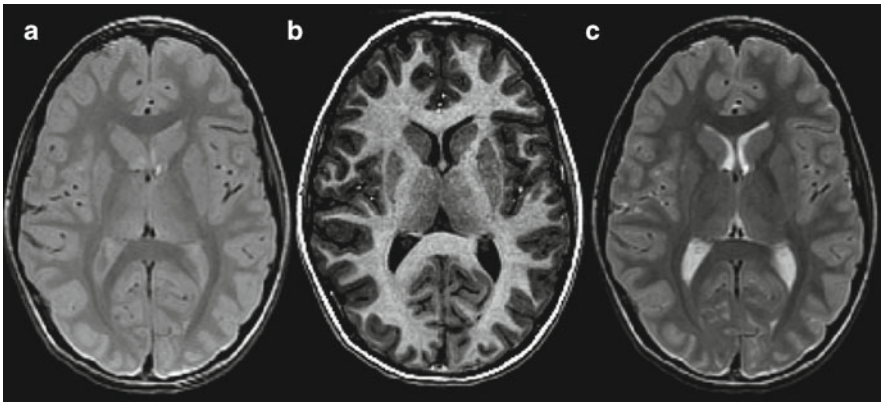

Fig. 1.16 MR Images in a healthy adult with respective weightings on proton density (**a**), T1 (**b**) and T2 (**c**)

Proton-density images, as the name implies, provide contrast based on the sheer number of protons in a voxel, which of course differs across tissue types. To maximize proton-density contrast, researchers use pulse sequences that minimize T_1 and T_2 contrasts. To minimize T_1 contrast, a complete recovery of longitudinal magnetization is needed, which requires a long repetition time (TR); to minimize T_2 contrast, no significant transverse decay is allowed, which requires a very short echo time (TE) to acquire image immediately after excitation.

Proton-density images can be used as high-resolution reference images for determining anatomical structure in the brain. For this reason, they are often an important part of fMRI studies. In addition, the tissue information they provide can be used to improve algorithms for segmenting brain structures on the basis of intensity values. Such segmentation approaches are often important when understanding how damage or atrophy in a region alters its functional properties, such as in the study of disease or aging. Proton-density images are frequently acquired at the same slice locations as T_1- or T_2-weighted images so that complementary anatomical information can be acquired, as shown in Fig. 1.16a.

1.4.5.2 T_1 Contrast

While proton-density images have many uses, other forms of contrast emphasize different features of the brain. One of the commonly used structural contrasts for anatomical images of the brain is T_1 weighting. Images are called T_1 weighted, if the relative signal intensity of voxels within the image depends upon the T_1 value of the tissue. To generate sufficient signal weighting on T_1 recovery, a moderate TR is required. As T_2 decay should be minimized to gain exclusive T_1 contrast, a very short TE is needed. In practice, T_1 weighted images are very useful for brain tissue visualization and segmentation, as it attenuates fluid (e.g. cerebrospinal fluid (CSF)) signal, and differentiates the gray and white matters, as shown in Fig. 1.16b.

To boost T_1 contrast, researchers often use a technique called inversion recovery, which begins the sequence with a 180° inversion pulse rather than the more common 90° pulse. Because the inversion pulse flips the net magnetization to the negative state, it effectively doubles the dynamic range of the signal. This in turn increases the maximal T_1 difference that can be measured between the tissues. Inversion recovery is also useful for selectively eliminating MR signal of a single tissue type. For example, when the magnetization of cerebrospinal fluid (CSF) is recovering from the inverted state to the original state, it will reach a point where there is no longitudinal magnetization (i.e. the zero-crossing point). If images are acquired at this point, there will be no signal from CSF in any voxel. The suppression of CSF allows better assessment of other tissue types, such as gray and white matter.

1.4.5.3 T_2 Contrast

Almost opposite to the T_1 contrast, by using T_2-contrast imaging, images can be created that have maximal signal in fluid-filled regions, which is important for many clinical considerations. Many tumors, arteriovenous malformations (AVMs), and other pathological conditions show up most readily under T_2 contrast. High-resolution T_2 images are also used as anatomical references in fMRI studies (an example is shown in Fig. 1.16c), either in isolation or in conjunction with proton-density or T_1 images in a multi-contrast segmentation algorithm. Thus, common clinical protocols include both T_1- and T_2-weighted images.

In order to allow exclusive T_2 weighting, the longitudinal magnetization needs to be fully recovered to remove any T_1 weighting, which requires a long TR. To remove the influence from unrelated factors such as the magnetic field inhomogeneity, a spin-echo pulse sequence (Hahn 1950), which uses a 180° pulse to refocus any static dephasing process, is usually employed to generate exclusive T_2 contrast. In practice, T_2 weighting is achieved by using a moderate TE, which allows for a moderate T_2 decay.

1.4.5.4 Susceptibility Contrast

MR signal can be influenced by the various susceptibilities of different materials. Susceptibility reflects how the materials are magnetized when placed in the magnetic field. As it is generally known, ferrous metals such as iron are easily magnetized and can retain their magnetism afterwards, making them contraindications for MRI. Many other non-ferrous substances, however, can have negative or positive susceptibility to magnetic fields, and be accordingly labeled as either diamagnetic or paramagnetic. Specifically, they would generate negative and positive magnetic fields when placed in an external magnetic field, but lose their magnetism when taken out the magnetic field. Materials with different susceptibilities disturb the uniformity of the main magnetic field, and can greatly alter MR signal intensities, especially when gradient echo or other T2* sensitive pulse sequences are used.

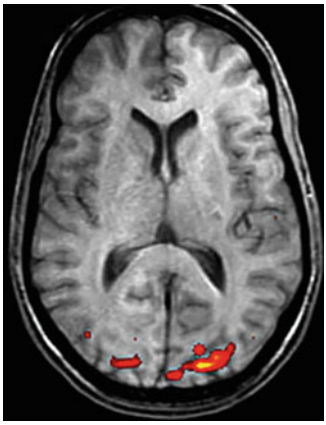

Fig. 1.17 An example of the BOLD signal localized in the primary visual cortex during visual stimulation

One of the primary examples of useful susceptibility contrast is the blood oxygenation level dependent (BOLD) signal (Ogawa et al. 1993) observed in functional MRI (fMRI). Because deoxyhemoglobin in blood is paramagnetic, the dynamic changes of its concentration modulate time-course MR signal intensities upon brain activation, giving rise to the dominant BOLD contrast that are widely used in fMRI research. Shown in Fig. 1.17 is a simple example of the functional BOLD signal in the primary visual cortex during visual stimulation.

While dynamic susceptibility contrast is useful in characterizing hemodynamic responses during brain function, static susceptibility can produce detailed images of brain vasculature. Recent results using susceptibility weighted imaging (SWI) (Haacke et al. 2004) have revealed exquisite details of the venous networks, with dominant contrast generated from the paramagnetic blood within the vasculature. More recent advances in susceptibility contrast at high field have further opened new possibilities to investigate the microanatomical structures of the human brain, with one of the new developments termed susceptibility tensor imaging (Liu 2010). Shown in Fig. 1.18 are three images of tensor element χ_{11}, χ_{23} and χ_{33} from an axial slice of a mouse brain at 7 T. The existence of off diagonal entries and the difference between diagonal entries are clear evidence of magnetic susceptibility anisotropy. The illustration of the brain susceptibility and its anisotropy may provide new ways to characterize the tissue molecular composition and orientation within the human brain.

1.4.5.5 Chemical Contrast

MR signal can also be made sensitive to the types of chemicals, and their concentrations, in the tissue, and thus contrast can be generated from this sensitivity. The principle of chemical contrast is based on the well-known phenomenon called chemical shift. Because protons experience different shielding effects from the surrounding electrons in different molecules, their resonance frequencies vary depending upon which type of molecule they are in. The chemical shift therefore reflects

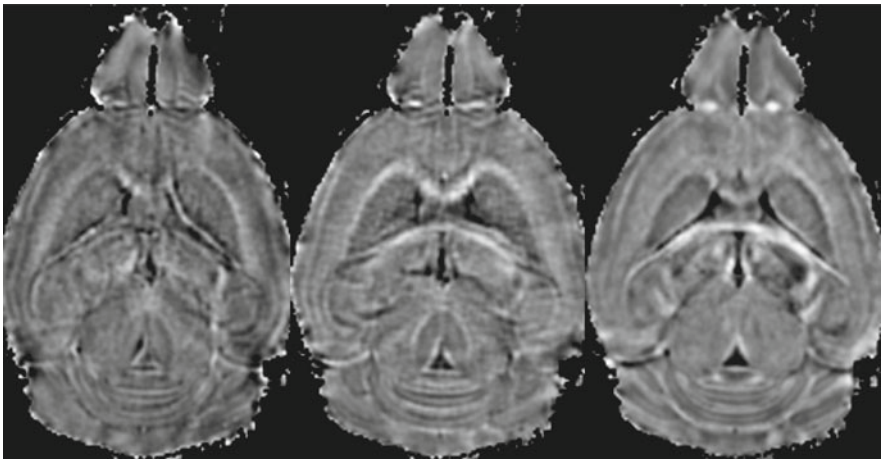

Fig. 1.18 Images of three tensor elements, χ_{11}, χ_{23} and χ_{33}, in an axial slice of a mouse brain at 7T, demonstrating the anisotropy in magnetic susceptibility of brain tissue

the difference in proton resonance frequencies in different molecules. For example, because protons in fat resonate at a slightly different frequency than those in water, targeted excitation can allow fat selection and fat suppression, which is a very useful practice in clinical MRI.

Chemical shift is also the basis of a different class of MR technique, termed **MR spectroscopy** (MRS), in which the small frequency difference among chemicals are investigated through MR spectra in the frequency domain. As a result, one may be able to quantify important metabolites in the brain such as N-acetyl aspartate (NAA, an index for neuronal viability), creatine (Cr), choline (Cho), Myoinositol (mI), etc. many of these substances play critical roles in regulating brain function, energetics, and metabolism. The ability to quantify these chemicals can be essential in brain function studies.

To resolve the subtle frequency differences of various metabolites, hundreds or thousands of data points are needed within each excitation, making it difficult to accommodate the time needed for spatial encoding. As such, early MRS was acquired in a single-voxel fashion, by using either point-resolved spectroscopy (PRESS) or stimulated echo acquisition mode (STEAM) techniques. Shown in Fig. 1.19 is an example of single-voxel MRS acquired using PRESS.

In recent years, with the improvement in hardware and software to accommodate both frequency and spatial resolutions without an excessively long acquisition time, new MRS techniques that allow for spatial differentiation of the metabolites have been developed. As a result, spatial maps known as chemical shift images (CSI) can be generated that reflect the concentrations of individual chemicals of interest in various regions of interest (Brown and Kincaid 1982).

While ^{1}H MRS has been dominant, other nuclei possessing NMR property (as discussed in earlier sections) can also generate signal. Indeed, recent developments in heteronuclear spectroscopy (e.g. ^{13}C, ^{31}P) have provided specific signal and assessment on cerebral energy metabolism and neurochemistry (Zhu et al. 2009).

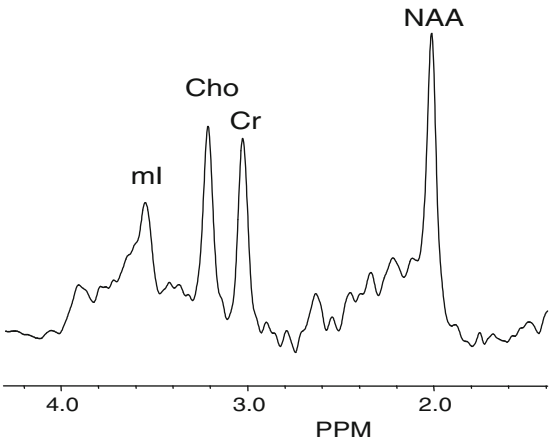

Fig. 1.19 Illustration of a MR spectrum using single-voxel PRESS acquisition, containing various metabolites of interest such as NAA, Cho, Cr, and mI

1.4.5.6 Macromolecular Contrast

In addition to the relaxational mechanisms (e.g. T_1 and T_2) that are based on the evolution of magnetization itself, contrast can also be generated based on the exchange among molecules. For example, the magnetization of the protons in macromolecules (e.g. proteins) can be transferred to those in water molecules, a phenomenon known as magnetization transfer. Many years after its first demonstration (Wolff and Balaban 1989), magnetization transfer is now widely used to generate contrast based on macromolecule concentrations.

The basic principle of magnetization transfer is based on the characteristics of the resonance frequencies of protons in different molecules, due to the various shielding effects of these molecules. In particular, the resonance frequency of protons within water molecules has a fairly narrow range, typically on the order of one hundred Hz; however, protons in macromolecules, albeit at a much lower concentration, can have a range of resonance frequencies that expand across several thousands of Hz. These two distinctly different frequency distributions allow selective excitation of some macromolecule protons, without exciting those in water. If adequate time (e.g. a few tens of milliseconds) is given, the magnetization of the protons in macromolecules will transfer into the protons in free water in the vicinity. If an excitation pulse is given after the transfer to image water, the overall signal in water will experience a reduction because some of the protons in the water already had magnetization from the macromolecules. Because the amount of magnetization transfer is directly proportional to the macromolecule concentration, the reduction seen in water signal can be used to infer macromolecular concentration.

Magnetization transfer contrast can have a significant clinical impact. For example, it can be used to detect changes in myelination in the brain and assess its effect on brain function, as myelin is physically a structure composed of macromolecules (e.g. phospholipids) (shown in Fig. 1.20 is a magnetization transfer-prepared image sensitive to myelin content). As such, magnetization transfer can often be used to

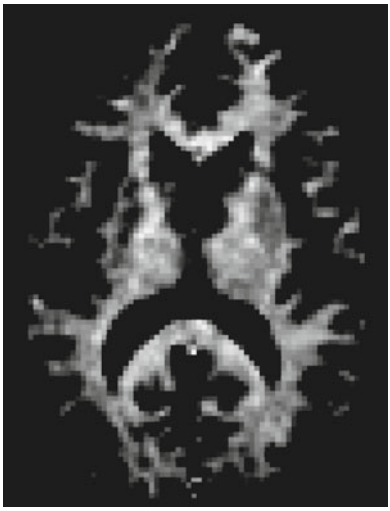

Fig. 1.20 Sample image of myelin content through macromolecular contrast using magnetization transfer

study maturation of myelin in pediatric brains, or investigate myelin disorders such as Multiple Sclerosis (e.g. demyelination) (Grossman 1999).

1.4.5.7 MR Angiography

Magnetic resonance angiography, or MRA, is a common motion-weighted contrast that illustrates the structure of blood vessels using noninvasive MRI. In classic angiography, a contrast agent is injected into the bloodstream through an inserted catheter. X-ray images are then collected with and without the contrast agent present to generate a difference image (i.e., angiogram) that maps the vascular system. Although angiography provides good vascular images, it is a very invasive procedure, requiring both the insertion of foreign substances and exposure to ionizing radiation. Because MRA does not require ionizing radiation, it can noninvasively detect, diagnose, and aid in the treatment of many types of medical problems, including cardiac disorders, stroke, and vascular disease. MRA also complements fMRI studies by identifying major blood vessels that may confound experimental results. If identified, these vessels can be removed from analyses to improve localization of activity to the capillary bed.

MRA can use either exogenous or endogenous contrast. In some clinical settings, exogenous contrast-enhancing agents are used to increase the vessel signal. For a typical contrast-enhanced MRA, a small quantity (or bolus) of a gadolinium-based contrast agent is injected into the patient's bloodstream. The gadolinium itself is not visible on MR images, but it radically shortens the T_1 of nearby blood, allowing the use of specialized pulse sequences with extremely short TR (3–7 ms) and TE (1–3 ms) values. The short TR saturates signal from stationary tissues but not from the gadolinium-enhanced blood, while the short TE minimizes T_2 decay. Depending on

Fig. 1.21 Sample image of MR angiogram using time-of-flight contrast

the delay between bolus injection and image acquisition, the contrast agent may travel through different components of the vascular system, so the images can be calibrated to provide information about arterial or venous networks.

In research settings, MRA is usually obtained using noninvasive endogenous contrast. There are two primary techniques for endogenous contrast MRA (see review by Haacke et al. 1991). The most common is time-of-flight (TOF) MRA, which generates signal based upon blood displacement. The underlying principle of the TOF technique is signal saturation. By repeatedly and frequently applying excitation pulses or gradient pulses to a single imaging plane, the signal within that plane can be suppressed. Thus, static tissues such as gray or white matter, will produce little MR signal and will appear to be very dark on TOF images. Blood vessels, however, are constantly replenished with new blood, hence new protons, from outside the plane. These protons have not experienced the excitation or gradient pulses, and thus they contribute normal MR signal. TOF images are typically acquired in the axial plane and can be reformatted to other planes for ease of viewing. An example of brain angiogram is shown in Fig. 1.21 based on TOF contrast.

A second technique is velocity-encoded phase contrast (VENC-PC) MRA, which uses gradient fields to produce a velocity-dependent phase difference between the vasculature and surrounding tissue. The amount of phase difference accumulated depends on the velocity of the moving blood and the strength and duration of the applied gradient. By acquiring phase differences in each of three orthogonal directions, a map of three-dimensional flow can be created. Typical VENC-PC protocols acquire two sets of images: one with a motion-sensitizing gradient and the other with either no gradient or a gradient in the opposite direction. The difference between these images indicates the magnitude of the phase difference at each voxel, and thus the brightness at each voxel is proportional to flow. Voxels with stationary tissue will not give signal, since there are no phase differences between the images, whereas voxels with rapidly moving blood will produce bright signals due to the large phase differences. The VENC-PC technique, unlike TOF, does not depend upon TR or slice thickness, because it acts upon the blood already present in the imaging slice.

1.4.5.8 Diffusion-Weighted Contrast

The random-walk motion of molecules due to thermodynamic effects is known as diffusion. In gases and liquids, the molecules can move relatively freely, as when a dye spreads through a glass of water or when the smell of freshly baked bread wafts through the house. In solids, however, the motion of molecules is restricted, and thus diffusion is much slower. The abundance of water molecules in the human body makes it possible to perform diffusion-weighted imaging using MRI (Stejskal and Tanner 1965). And, because of the different cellular environment experienced by different water molecules, diffusion-weighted MRI can provide a new dimension of image contrast based on mobility.

Diffusion weighting is the application of controlled gradient magnetic fields to quantify the amplitude and direction of diffusion. The presence of diffusion-weighting gradients further attenuates the MR signal beyond that caused by common T_2 relaxation. Assuming equal, or isotropic, diffusion along all directions, the attenuation effect (A) due to diffusion weighting is given by equation $A = e^{-bD}$, here D is the apparent diffusion coefficient, or ADC, b defines the severity of diffusion weighting (which is governed by the duration and amplitude of the diffusion weighting gradients).

Water molecules in the brain do not always diffuse equally in all directions. In fact, most water is contained within tissue that has considerable structure, such as the long processes of axons or the narrow walls of blood vessels. Unequal, or anisotropic, diffusion refers to the preference in some tissues for water molecules to diffuse in one direction or another. In anisotropic diffusion, the motion of molecules over time does not resemble a sphere, in which molecules move equally in every direction, but instead resembles an ellipsoid whose long axis indicates the fastest axis of diffusion. The diffusion ellipsoid is mathematically described as a three-dimensional tensor (Basser et al. 1994), which is a collection of vector fields governed by three principal axes. One useful image derived from the diffusion tensor is the fractional anisotropy map, which reflects the degree of anisotropy from 0 to 1, with 0 being isotropic, for each voxel. A color coded example of fractional anisotropy map is shown in Fig. 1.22, illustrating the degree of anisotropy (intensity) and directionality (color). The field of diffusion tensor imaging (DTI) has seen marked growth in the past decade as it provides a new way to study structural connectivity of white matter and delineate nerve fiber tracts (Mori et al. 1999).

1.4.5.9 Perfusion-Weighted Contrast

To ensure a constant supply of oxygen, hemoglobin molecules carry oxygen through the bloodstream to tissue and organs (e.g. brain). The irrigation of tissue via blood delivery is known as perfusion, and the family of imaging procedures that measure this process are known as perfusion MRI. Perfusion is expressed as the volume of blood that travels through a tissue mass over time. Unlike the MRA techniques described in the previous section (which are often used for clinical reasons to measure

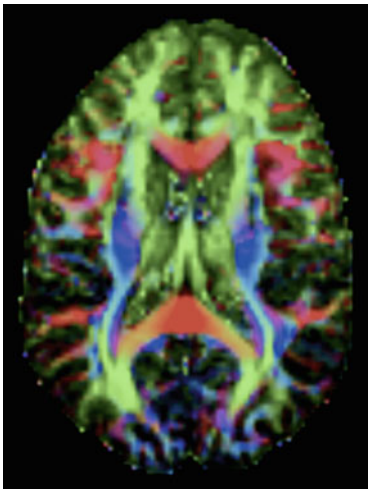

Fig. 1.22 Sample image of fractional anisotropy using diffusion tensor imaging, directionality is color coded (*red*: left – right; *blue*: superior – inferior; *green*: anterior – posterior)

the properties of large blood vessels), perfusion MRI is most frequently used to image blood flow specifically in capillaries and other small vessels.

Similar to MRA, perfusion MRI may use either exogenous or endogenous contrast. Exogenous contrast approaches use intravascular contrast agents that freely perfuse through the vascular system (See review by Prince and Body 1996). The attenuation of the MR signal in each voxel is proportional to the amount of the contrast agent present. Thus, signal changes can be interpreted as a function of perfusion, and images can be created that depict different perfusion properties, such as the relative cerebral blood flow (rCBF), relative cerebral blood volume (rCBV), and mean transit time (mTT). As their names imply, relative blood flow and relative blood volume express changes in how much blood comes into a voxel and how much blood is contained within a voxel, respectively. The mean transit time measures how quickly blood passes through a particular voxel and can indicate brain regions with delayed blood flow. The use of exogenous contrast agents provides very high signal change but has limited use for research because of its invasiveness.

Endogeneous contrast perfusion imaging is noninvasive and has found use in fMRI research. Contrast is generated through the clever use of radiofrequency pulses to magnetically label protons in blood water molecules before they reach the tissue of interest (Detre et al. 1992). This approach is known as arterial spin labeling, or ASL, of which there are two types: continuous and pulsed. Continuous ASL typically uses additional hardware, like a labeling coil, to saturate spins in upstream blood, such as in the carotid arteries of the neck. Following this labeling process, the blood travels to the brain and enters the imaging slice. The images can then be continuously acquired in the brain in the presence of the labeled blood. A drawback of the continuous ASL technique is the requirement for a second transmitter coil to label the inflowing blood. Pulsed ASL uses a single coil both to label blood in a distal labeling plane and to record the MR signal change in the imaging plane.

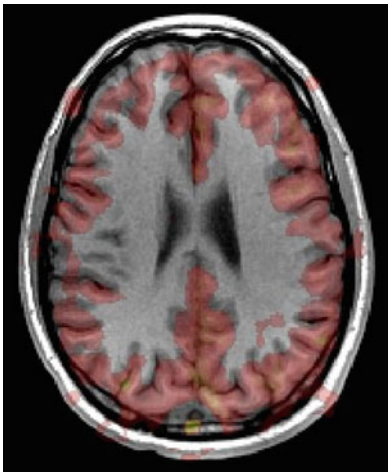

Fig. 1.23 Sample image of perfusion map (in *translucent red*) using pulsed arterial spin labeling

Labeling pulses are broadcast for brief periods and followed by a delay and then image acquisition. The delay period must be calibrated to account for the distance between the labeling plane and imaging plane, so the labeled bolus of blood water will enter the imaging plane during image acquisition and produce quantitative perfusion image (Wong et al. 1998) only related to the labeled blood water, as shown in translucent color in Fig. 1.23.

References

Basser PJ, Mattiello J, Le Bihan D (1994) Estimation of the effective self-diffusion tensor from the NMR spin echo. J Magn Reson B103:247–254

Bloch F (1946) Nuclear induction. Phys Rev 70:460

Brown TR, Kincaid BM (1982) Ugurbil, NMR chemical shift imaging in three dimensions. Proc Natl Acad Sci USA 79(11):3523–3526

Damadian R (1971) Tumor detection by nuclear magnetic resonance. Science 171:1151

Detre J, Leigh JS, Williams DS, Koretsky AP (1992) Perfusion imaging. Magn Reson Med 23(1):37–45

Ernst RR, Bodenhausen G, Wokaun A (1987) Principles of nuclear magnetic resonance in one and two dimensions. Oxford, New York

Grossman RI (1999) Application of magnetization transfer imaging to multiple sclerosis. Neurology 53(5 Suppl 3):S8–S11

Haacke EM, Smith AS, Lin W, Lewin JS, Finelli DA, Duerk JL (1991) Velocity quantification in magnetic resonance imaging. Top Magn Reson Imaging 3(3):34–39

Haacke EM, Brown RW, Thompson MR, Venkatesan R (1999) Magnetic resonance imaging: physical principles and sequence design. Wiley-Liss, New York

Haacke EM, Xu Y, Cheng YC, Reichenbach JR (2004) Susceptibility weighted imaging (SWI). Magn Reson Med 52:612–618

Hahn EL (1950) Spin echoes. Phys Rev 80:580

Lauterbur PC (1973) Image formation by induced local interactions: examples employing NMR. Nature 242:190

Liu C (2010) Susceptibility tensor imaging. Magn Reson Med 63:1471–1477
Mansfield P (1977) Multi-planar image formation using NMR spin echoes. J Phys C 10:L55
Mori S, Crain BJ, Chacko VP, Van Zijl PCM (1999) Three-dimensional tracking of axonal projections in the brain by magnetic resonance imaging. Annal Neurol 45(2):265–269
Ogawa S, Menon RS, Tank DW, Kim SG, Merkle H, Ellermann JM, Ugurbil K (1993) Functional brain mapping by blood oxygenation level-dependent contrast magnetic resonance imaging. A comparison of signal characteristics with a biophysical model. Biophys J 64(3):803–812
Prince MR, Body MR (1996) angiography with gadolinium contrast agents. Magn Reson Imaging Clin N Am 4(1):11–24
Purcell EM, Torrey HC, Pound RV (1946) Resonance absorption by nuclear magnetic moments in a solid. Phys Rev 69:37
Rabi II, Zacharias JR, Millman S, Kusch P (1938) A new method of measuring nuclear magnetic moments. Phys Rev 53:318
Stark DD, Bradley WG (1992) Magnetic resonance imaging, Mosby-Year Book
Stejskal EO, Tanner JE (1965) Spin diffusion measurements: spin echoes in the presence of a time-dependent field gradient. J Chem Phys 42(1):288–292
Wolff SD, Balaban RS (1989) Magnetization transfer contrast (MTC) and tissue water proton relaxation in vivo. Magn Reson Med 10(1):135–144
Wong EC, Buxton RB, Frank LR (1998) Quantitative imaging of perfusion using a single subtraction (QUIPSS and QUIPSS II). Magn Reson Med 39:702–708
Zhu XH, Zhang N, Zhang Y, Lei H, Zhang X, Qiao H, Ugurbil K, Chen W (2009) Advanced in vivo heteronuclear MRS approaches for studying brain bioenergetics driven by mitochondria. Methods Mol Biol 489:317–357